



NIMFEIA

Deliverable D6.1

Report on benchmark of magnon reservoir on NARMA data

Project number	101070290
Project name	Nonlinear Magnons for Reservoir Computing in Reciprocal Space
Project acronym	NIMFEIA
Work package	WP 6.1
Type	Report
Dissemination level	Public
Lead beneficiary	Radboud University
Due date of delivery	24

Authors: Thomas Brian Winkler, Johan H. Mentink

Disclaimer:

The NIMFEIA project has received funding by the European Union's Research and Innovation Programme Horizon Europe under grant agreement No 101070290. However, views and opinions expressed in this document are those of the authors only and do not necessarily reflect those of the European Union. The European Union cannot be held responsible for them.

1. Introduction

1.1. Motivation

Very recently, skyrmion-based Reservoir computing was successfully demonstrated by NIM-FEIA consortium members [1,2]. Combined temporal and spatial multiplexed skyrmion trajectories were analyzed to distinguish different types of gestures (such as *push*, *swipe left/right*), obtained by radar data. In an even earlier study on a similar confined skyrmion device, non-separable logic gates, such as the NAND or the XOR-gate were also realized by spatial multiplexing. As a next step, we want to try time series prediction with the skyrmion reservoir.

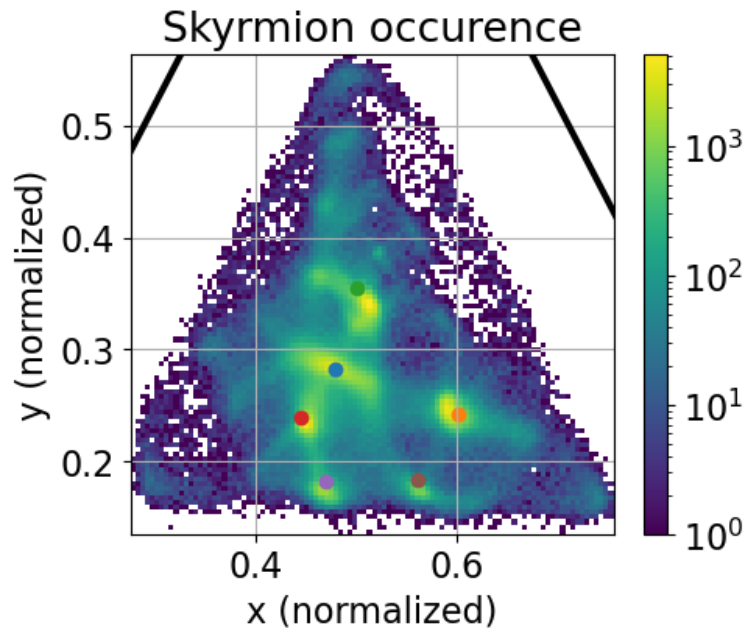


Figure 1: Skyrmion occurrence map and the color-code of the pinning sites. The color scale visualizes skyrmion counts at the respective position.

1.2. Markov State Modeling

Compared to classical Reservoir computing approaches, Brownian Reservoir computing leverages stochasticity. Exploiting skyrmion diffusion in a single-layer *CoFeB* skyrmion stack, as used in previous studies, allows for ultra-low current operation and the ability to overcome pinning effects.

However, the effective energy landscape of the sample due to inhomogeneities in the material is apparent. The skyrmions trajectory under a current input (which encode the time series signal) is still hopping-dominated. Illustratively, **Figure 1** shows the occurrence map of a skyrmion (multiple measurements were stacked for a clear visualization of the effective energy landscape) with only a few (yellow) pinning sites, in which the skyrmion likes to stay most of the time (the data was acquired by optical Kerr microscopy). This discretization possibility motivates the modeling of the skyrmion system as a Markovian process, giving us the opportunity to analyze the memory capabilities and stochastic properties within the description of Markov processes. The magnetic system is coarse-grained into K reasonable skyrmion pinning sites. A transition matrix \tilde{T} is obtained from long-term measurement under fixed conditions (i.e. no



change of applied voltage or magnetic field condition), in our case we scan the applied voltage in a reasonable range (in which the skyrmion annihilation probability at the device boundaries is negligible) with 5 measurements, $-1.5 \text{ mV} \leq U \leq 2 \text{ mV}$. **Figure 2** show skyrmion occurrence of long-term measurements for different applied voltages (used contacts are at the top and the bottom right corner of the triangle, the bottom left corner is left free – no applied voltage).

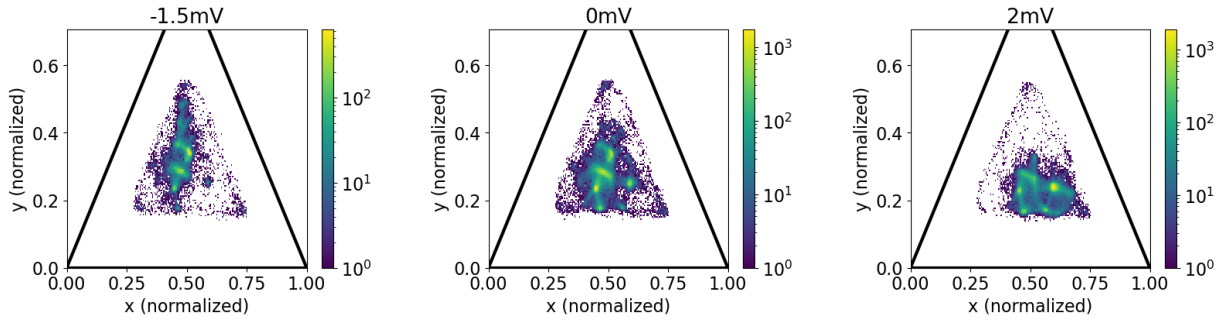


Figure 2: Skyrmion occurrence map for different applied voltages. Under applied voltage, the skyrmion is driven by spin-orbit torque in the direction to one of the electrodes, depending on the sign of the voltage. The color scale visualizes skyrmion counts at the respective position.

Each entry t_{ij} of a transition matrix \mathbf{T} is the conditional probability for a skyrmion hopping from pinning site i to pinning site j .

The transition matrix is the heart of a Markov State Model (MSM) and allows us for example to:

- 1.) To “time-integrate” a system by lag time τ , which can be given as a distribution \mathbf{p} , with p_i the probability of being in pinning site i , and $\sum_{i=0}^{K-1} p_i = 1$.
- 2.) Calculate a stationary distribution $\boldsymbol{\pi}$, which does not change when \mathbf{T} is applied.
- 3.) Estimate “memory” of our skyrmion reservoir and intrinsic time scales of the hopping.

The goal is to run ultra-fast predictions of our skyrmion reservoir device. Once the model is obtained, we numerically integrate in time steps of the microscopy’s framerate (in our case 16 Hz), which is orders of magnitude higher than possible with micromagnetic or Thiele-based simulations. Next, we aim for experimental verification of predictions of our skyrmion reservoir MSM. Finally, we use the model to test performance on the NARMA data set.

1.3. Energy Modeling

To scale transition matrices and stationary distributions continuously for any applied voltages, we model the system as follows:

1. An energy is assigned to each pinning site, with respective linear scaling with applied voltage: $E_i(U) = E_i^0 + c_i \cdot U$. The voltage-dependent stationary distribution is then



given by $\boldsymbol{\pi}(U) = \text{SOFTMIN}(\mathbf{E}(U)) = \frac{\exp(-E(U))}{\sum_{k=0}^{K-1} \exp(-E_k(U))}$, a discrete analogy of the Boltzmann distribution.

2. Further an energy is assigned to each transition $i \rightarrow j$, $E_{ij} = E_{ij}^0 + c_{ij} \cdot U$, again with linear voltage scaling. The effective energy barriers from state i , $\Delta E_i(U)$ (with entries $\Delta E_{ij}(U) = E_{ij}(U) - E_i(U)$) is used to calculate the i -th row of the transition matrix $\mathbf{T}_i = \text{SOFTMIN}(\Delta E_i(U))$, adapting the procedure for the stationary distribution. The exponential scaling with energy is also apparent in the Arrhenius law, while the attempt frequency is neglected in our approach.

We minimize the problems numerically with least-squares loss to fit energies and voltage scaling factor to our device (as initial values we use estimations based on experimental data $\tilde{\mathbf{T}}$, for the current scaling we run current path simulations). **Figure 3** shows the modeled distributions (**left**) and transition rates (**right**), as well as the data obtained from experiment. We find good agreement for both the stationary distribution and the transition rates.

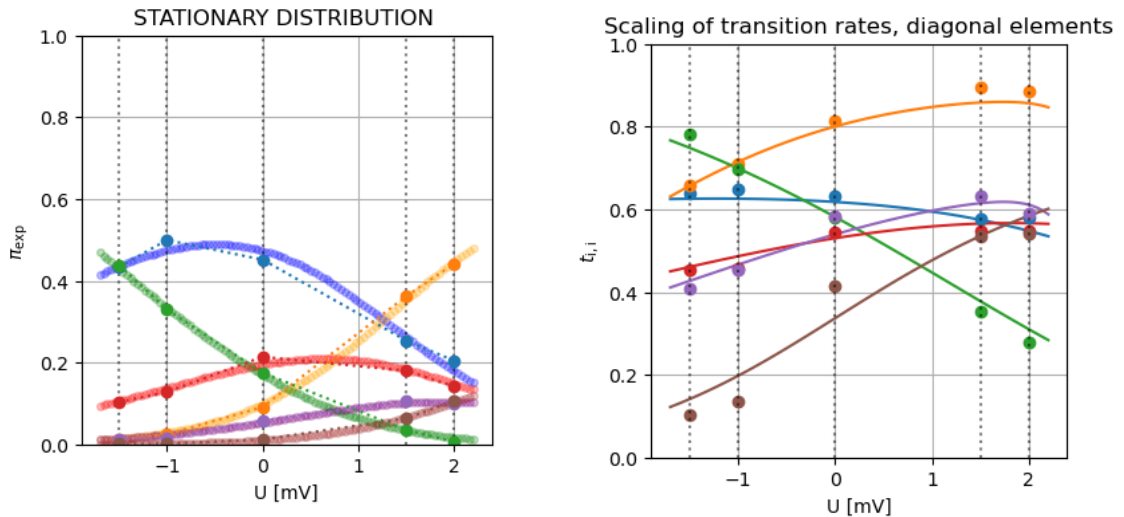


Figure 3: Modeled (curves) and measured (points) stationary distribution – left – and transition rates of the matrix diagonal – right – showing good agreement.

2. Time series forecasting with Markov State modeled skyrmion device

The modeled skyrmion reservoir can now be driven by a voltage signal. We use the (non-linear auto-regressive moving average) NARMA as use case. The time series can be constructed by $y_t = \alpha y_{t-1} + \beta y_{t-1} \sum_{i=1}^n y_{t-i} + \gamma u_{t-n} u_{t-1} + \delta$, with $n = 10, \alpha = 0.3, \beta = 0.05, \gamma = 1.5, \delta = 0.1, u \in [0, 0.5]$ is uniform noise. The formulas imply that n previous steps are required to construct the next time step of the series. A time series of 1000 time steps is plotted in **Figure 4**. We linearly map the noise range $u \in [0, 0.5]$ to a reasonable voltage range of our MSM model, chosen with $U_{min} = -1.7$ mV, $U_{max} = 2.2$ mV.



Our reservoir system s is initialized with the stationary distribution of the mean value of the noise in the data set $\pi(U(\bar{u}))$. Then, we drive the system with the time signal, converted into a voltage signal. Each timestep in the NARMA signal coincides with the lag time τ of the MSM.

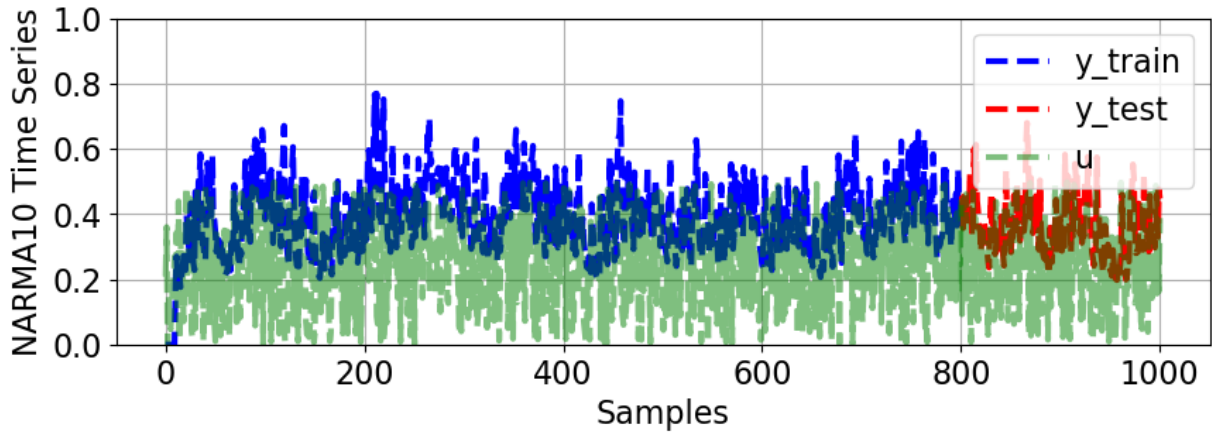


Figure 4: NARMA dataset for given parameters. 1000 steps are separated into training and test set.

Figure 5 illustrates the response of the Reservoir under the injection of the voltage series.

We train a linear model $\theta(s_{t-1}, \dots, s_{t-n}, u_{t-1}, \dots, u_{t-n})$ on the last n time steps to predict the next output y . The predictive power of the reservoir is evaluated by the normalized root mean square error $\text{NRMSE} = \frac{\sqrt{\langle (y - \hat{y})^2 \rangle}}{\hat{y}_{\max} - \hat{y}_{\min}}$. We find $\text{NRMSE}_{\text{train}} = 0.727$, in the training range and $\text{NRMSE}_{\text{test}} = 0.828$ in the testing range of the data set. Figure 6 compares the output y with the predicted one y_{pred} .

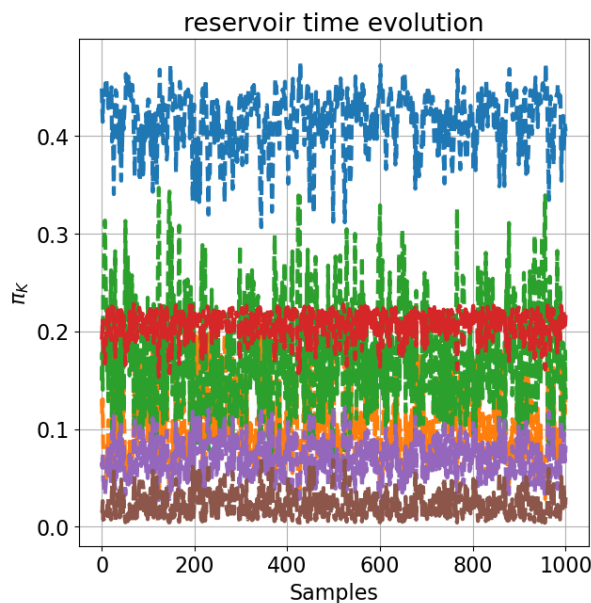


Figure 5: The time evolution of the reservoir under the applied voltage signal. The color indicates the pinning site, as visible in Figure 1.



As next steps, we can analyze the performance of the reservoir, when actual skyrmion trajectories are sampled (instead of working in the limit of infinite statistics). Also, we can try to improve the results by adjusting the mapping between noise u and voltage U as well as between the lag time τ and one time step of the NARMA series.

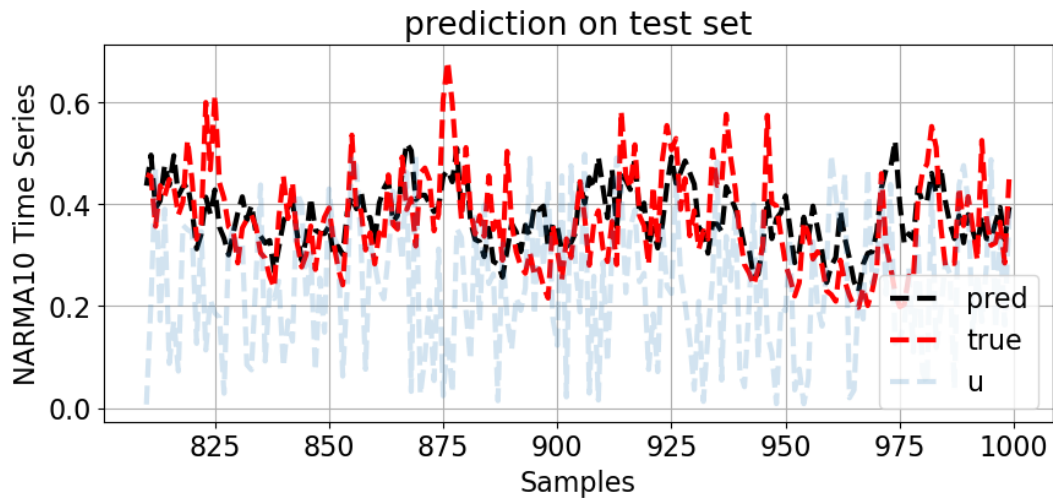


Figure 6: True versus predicted y in the test set.

3. Bibliography

- [1] G. Beneke, T. B. Winkler, K. Raab, M. A. Brems, F. Kammerbauer, P. Gerhards, K. Knobloch, S. Krishnia, J. H. Mentink, and M. Kläui, Gesture recognition with Brownian reservoir computing using geometrically confined skyrmion dynamics, *Nat Commun* **15**, 8103 (2024).
- [2] K. Raab, M. A. Brems, G. Beneke, T. Dohi, J. Rothörl, F. Kammerbauer, J. H. Mentink, and M. Kläui, Brownian reservoir computing realized using geometrically confined skyrmion dynamics, *Nat Commun* **13**, 6982 (2022).

